

# Thermal Interface for Pluggable Optics Modules

By Bonnie Mack, Senior Thermal Engineer and Terence Graham,  
Senior Thermal Engineer, Ciena Corporation

**ciena**  
Experience. Outcomes.



**P**ower on pluggable optics modules (POMs) such as SFP+, QSFP+, QSFP28, CFP2, CFP8 has increased along with the demand for higher bandwidth. POMs give access at the faceplate to an optical signal. Existing Multi-Source Agreements (MSAs) specify physical form factor and electrical interfaces, which allow multiple manufacturers to make physically compatible products to promote competition, interoperability and multiple sources for systems vendors and end users. These MSAs also define power classes for POMs that are based on the supplied power and correspond to different internal processing levels and optical signal reach. POMs are designed to support various communication standards and their data rates range from ~1 Gb/s to 400 Gb/s with many data rates available in each form factor.

POMs are difficult to cool; all but the CFP, are housed in a cage which guides the modules to the connectors and contains EMC solutions for the faceplate ports. The modules extend through the faceplate, and can be hot swapped. There are air gaps, ~0.2mm to 0.3mm nominal, between the module case and the cage, and between the cage and PCB. This provides an inconsistent thermal resistance due to tolerances. The cages generally have small openings on the sides to allow ingress and egress of air for cooling purposes. With high power POMs, these openings do not provide sufficient cooling so an opening on the cage top is added which gives access for a spring-loaded riding heatsink. To date only a dry thermal interface between the two surfaces has been available because the pluggable feature has precluded the use of thermal interface materials between the heatsink and the POM case. The thermal interface between POM and heatsink is not consistently defined or controlled in the MSAs. The challenge is to permit the required sliding while providing a low interface thermal resistance. This is especially important in a telecom environment where equipment in NEBS [1] shelf level products must operate in an ambient of 55°C. POMs temperature case limit is usually 70°C. This results in a 15°C temperature delta to cool the POMs, usually less when pre-heated by other POMs or components. Figure 1 shows typical

thermally-important features of POMs and cages.

Heat transfer routes to and from the POMs are described in references [2,3]. Thermal evaluation requires detailed 3D conjugate heat transfer analysis software. Essential input for the analyses includes detailed geometric, power, and thermal properties of the POM, EMC gasket and cage, and contact interface as described in the OIF thermal interface specification IA# OIF-Thermal-01.0 [4].

IA# OIF-Thermal-01.0 specifies general resistance parameters for the thermal interface as a function of power density. For high power modules, the major path for heat removal is via the heatsink across the contact area with the POM. It stipulates the MSA to define the location and size of contact area for heat removal on the top surface of POM. It also describes factors affecting thermal interface resistance: flatness, surface finish, and heat spreading. Additionally, it defines a calibration method for the internal sensors and includes the requirement to identify the location of thermal monitor point(s).

The initial work done in support of IA# OIF-Thermal-01.0 IA included a study of the thermal interface resistance between a CFP2 lid and heatsink base including heat spreading effects. The study examined three contact

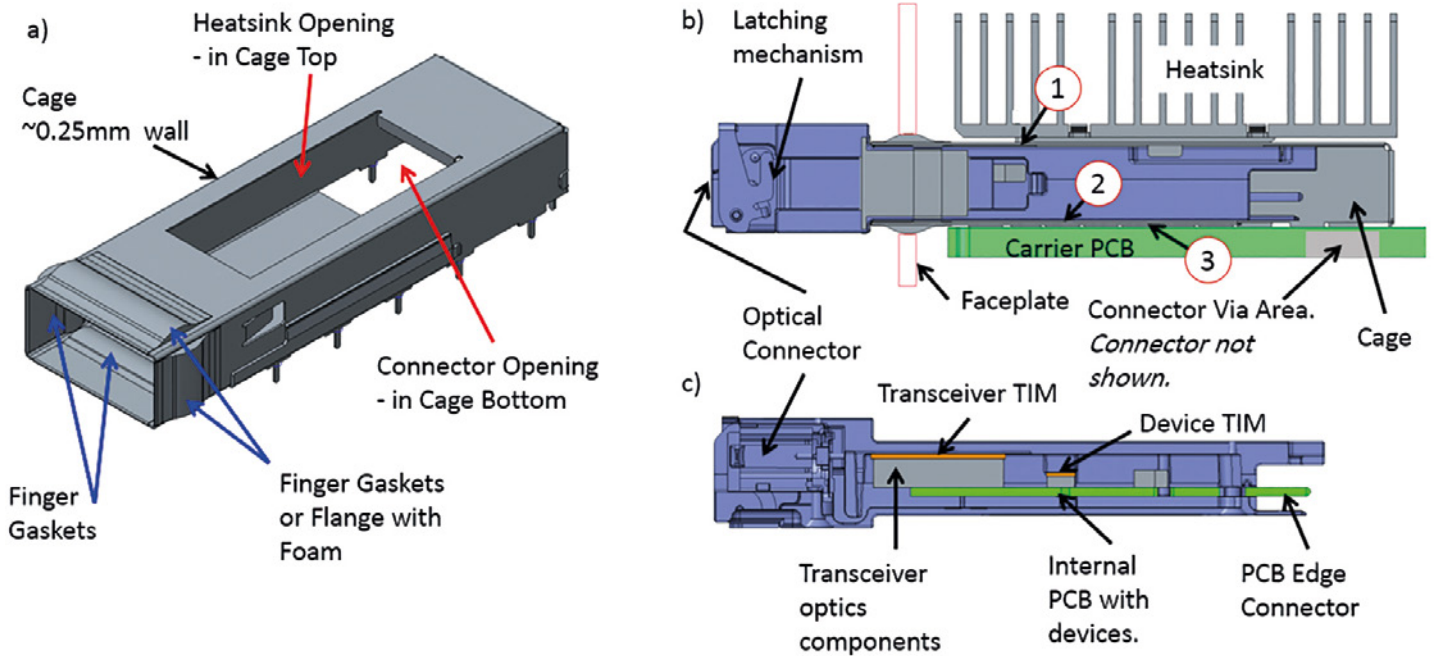


**Figure 1.** a) A typical POM cage, b) QSFP in cage section at inside edge of cage, c) QSFP section showing typical internal layout. Narrow air gap locations: 1) Module to top of cage, 2) Module to bottom of cage, 3) Bottom of cage to PCB, and not shown 4) sides of module to sides of cage.

scenarios: 1) a transverse bump in the center of the lid, 2) a transverse hollow in the center of the lid, and 3) a transverse contact in the center and ends of the lid. All three scenarios have the same contact area. These simplified contact geometries are depicted in Figure 2 and the contact gap ranges from what would be an extremely fine production surface flatness to 0.3mm, the maximum allowed by the MSA for the CFP2 contact surface for Power Class 1 and 2. It was assumed for the study that both surfaces had the same type of out of flatness so that modeling of the net gap between surfaces was easily implemented in FloTHERM® software used for the analysis.

The resistance in the contact areas between the heatsink and the module was modeled using the method described by Yovanovich et al. [5]. Where:

$$\text{Joint Resistance } h_j = h_{\text{contact}} + h_{\text{gap}}$$

A simplified CFP2 FloTHERM model was created with a T6063 aluminum case and up to six sources that can be set to dissipate power and to contact the lid as shown in Figure 3. Results were obtained for varying gaps due to out-of-flatness and different source locations. Intake air is 55°C at 1m/s across the enclosure cross-section upstream of the module. Total power for the CFP2 is 12W in all cases. Other model details are given in [2,3]. CFP2 lid temperature is monitored directly above the center of each source. Maximum lid temperatures are plotted in Figure 4 versus net flatness over the range

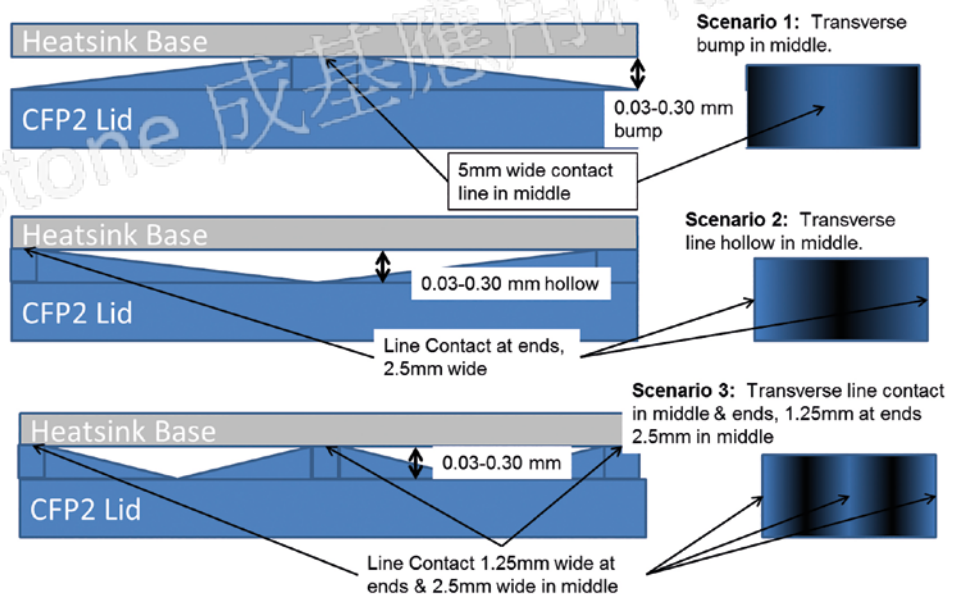


**Figure 2.** CFP2 Contact Interface Flatness Scenarios

of 0.03 mm to 0.3 mm flatness, for the three scenarios depicted in Figure 2.

Defining:

- $T_{\text{Lid max}}$  = maximum lid temperature
- $T_{\text{HS ave}}$  = average heatsink pad temperature
- $dT_{\text{Lid}}$  = temperature difference among lid locations A – F (indicative of thermal spreading resistance)
- $dT_{\text{Lid max to HS ave}} = T_{\text{Lid max}} - T_{\text{HS ave}}$

Spreading resistance in the lid was highest for scenario one, a center bump, which is

also effectively a single contact. Spreading resistance varies with the thermal conductivity and thickness of the lid. The interface resistance between the lid and heatsink is shown to be sensitive to the interface flatness. Temperature differences between lid and heatsink base can be reduced by 5°C to 8.5°C with flatness improvement on a CFP2 depending on heat source location and the nature of the out-of-flatness. This is a third to half of the CFP2 temperature budget in a NEBS environment! This is a huge improvement without increasing the size of the heatsink.

**QSFP Model – Expanding on the Effect of Spreading Resistance**

The QSFP form factor is a common POM that presently has the highest power density of all the form factors. Most of its heat is dissipated close to the faceplate and not directly underneath the heatsink contact area. A numerical wind tunnel study was conducted to explore the internal resistances and develop methods of reducing the QSFP temperatures. The numerical model, detailed in [2,6], was similar to that of [7] having a 5 W QSFP and a power density of 1.34 W/cm<sup>2</sup>, class pd14. Cooling was via a typical aluminum off-the-shelf heatsink. The model was used to predict the effect of changes in the heat source locations relative to the heatsink contact area and surface finish in the interface area. Figure 5 gives the scenario descriptions. For scenario d) the 5mm extension of the heatsink contact area towards the transceivers, the power density decreases 15% to 1.14 W/cm<sup>2</sup> or to pd12. Two contact resistance values between the case and the heatsink were explored as well for two difference surface roughness and load conditions. Results were calculated for QSFP case material thermal conductivities of 116, 169, 385 and 1000 W/m-K corresponding to a zinc alloy, high grade aluminum casting, copper, and an ultra-high conductivity material respectively. FloTHERM Command Centre was used to solve these scenarios.

The results shown in Figure 6 illustrate the importance of the surface finish of the case and heatsink, and of locating the heat sources and the thermal interface area as closely together as possible. QSFP MSA cage dimensions [8-9] allow an increase in heatsink contact length by up to 5mm. In our model this larger contact resulted in a temperature decrease of more than 1.5°C with the lowest case conductivity and Rc1. If the case material conductivity is increased to 169 or 385 W/m-K, further decreases of 1°C to 2°C respectively could be achieved. While very high case conductivities representing an exotic material was examined, changing QSFP case material to Cu from zinc

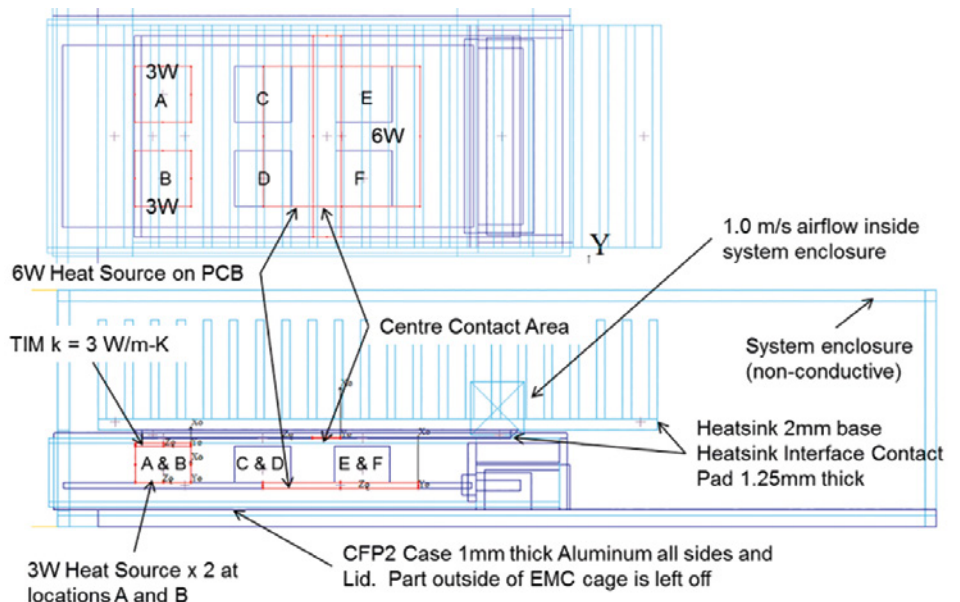


Figure 3. CFP2 flatness model layout showing front device, rear CFP2 PCB heat and central contact location

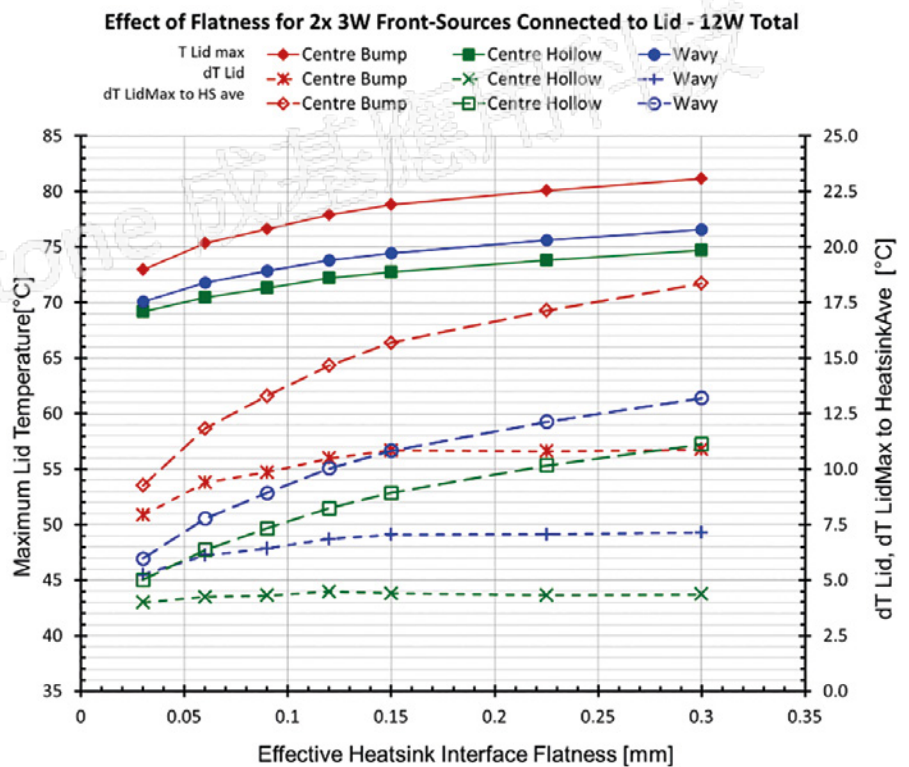
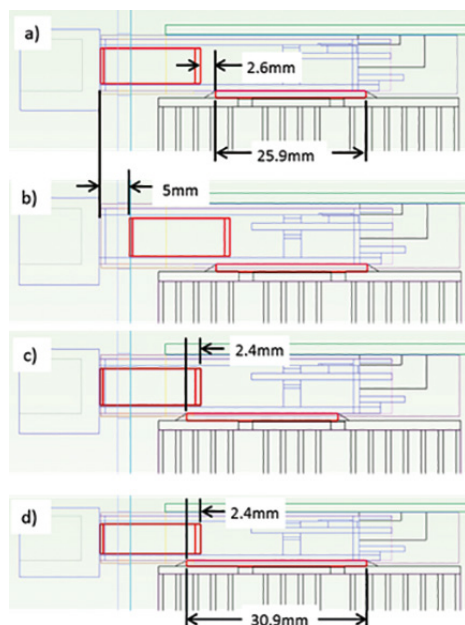


Figure 4. Range of flatness results with front device, and rear PCB heat dissipation and only the devices connected directly to the lid.

alloy can improve performance by 2 to 3°C. Decreasing the contact resistance to Rc2 would bring total improvement to ~5°C. These are significant when the overall ambient to case temperature budget could be 15°C or less.

The expansion of the heatsink opening in the cage has been incorporated into the MSA for the much higher power QSFP-DD modules [10].



**Figure 5.** Modeling scenarios for the QSFP a) Original, b) Transceivers 5 mm closer to heatsink contact, c) Heatsink contact 5 mm closer to transceivers, d) Heatsink contact 5 mm longer towards transceivers. Transceiver location is the red rectangle on the left.

Final module thermal assessment is at present only available with a computationally expensive detailed model created from the information specified in [4] and either built by the system designer with information from the module supplier, or is a model supplied by the module vendor, likely under some type of non-disclosure agreement. An alternative to this that has not yet been explored is the development of a Delphi-type resistance network. A model of this type could be used to model the connections to the PCB, surrounding air and heatsink with distributed internal heat sources in a manner similar to that used for multi-junction integrated circuit devices. This could be provided by module vendors without giving internal details of the module.

#### References:

- [1] Telcordia Technologies Generic Requirements, Generic Requirements for Telecommunications Data Center Equipment and Spaces, GR-3160-CORE, Issue 2, July 2013
- [2] Mack, B., Graham, T., Thermal Specifications for Pluggable Optics Modules, 32 IEEE SEMI-THERM Symposium, March 2016.
- [3] Mack, B., Graham, T., Pluggable Optics Module – Thermal Specifications, Part 1, Electronics Cooling, June 2016.
- [4] IA# OIF-Thermal-01.0, Implementation

#### Lid Hot Spot to Heatsink Temperature Difference

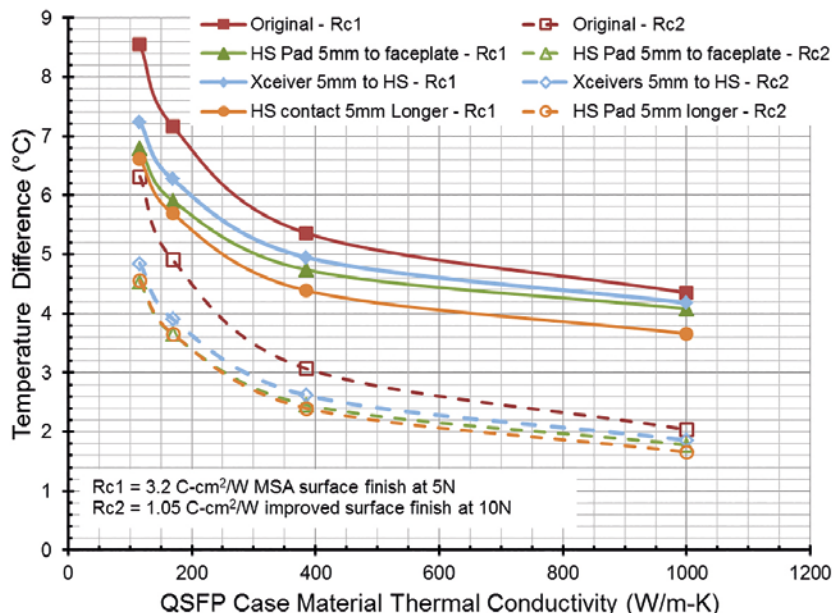


**Figure 6.** Temperature difference between QSFP hot spot monitor point and heatsink pad. Surface finishes of  $0.6 \mu\text{m Ra}$  and  $1.6 \mu\text{m Ra}$  on both heatsink and case

Agreement for Thermal Interface Specification for Pluggable Optics Modules, Optical Internetworking Forum, May 18, 2015

- [5] Yovanovitch, M.M., Culham, J.R., and Teerstra, P., Calculating Interface Resistance, Electronics Cooling, Article 3, May 1997, [http://www.electronics-cooling.com/Resources/EC\\_Articles/May97/article3.htm](http://www.electronics-cooling.com/Resources/EC_Articles/May97/article3.htm)
- [6] Graham, T., Mack, B., Pluggable Optics Module – Thermal Specifications, Part 2, Electronics Cooling, September 2016.
- [7] OIF-PLUG-Thermal-01.0, Thermal Management at the Faceplate White Paper, Optical Internetworking Forum, March 2012
- [8] SFF Committee, SFF-8663 Specification for QSFP+ 28 Gb/s Cage (Style A), Rev 1.5 April 2014, <ftp://ftp.seagate.com/sff>
- [9] SFF Committee, SFF-8661 Specification for QSFP+ 28 Gb/s 4x Pluggable Module, Revision 2.0, February 2014, <ftp://ftp.seagate.com/sff>
- [10] Quad Small Form Factor Pluggable Double Density (QSFP-DD) Multi Source Agreement (MSA) Group, QSFP-DD 3.0 Hardware Specification, September 2017 [www.qsfp-dd.com](http://www.qsfp-dd.com)



**Mentor**  
A Siemens Business

This article originally appeared in Engineering Edge Vol. 7 Iss. 1

Download the latest issue:  
[www.mentor.com/products/mechanical/engineering-edge](http://www.mentor.com/products/mechanical/engineering-edge)

# ENGINEERING EDGE

Accelerate Innovation  
with CFD & Thermal  
Characterization

## You might also be interested in...

**Thermal Simulation of a SYN TRAC Powerpack**

**Edge Devices are Hot for IoT**

**Distributed Chilled Water Pumping AC System**

**Reliability Evaluation of Sintered Copper Die Bonding Materials**

**Virtual Reality and Modeling Tools**

**Ask the GSS Expert**

**Simulation of Hydraulic Servo Gimbal Control of a Space Launch Vehicle**

**How to... Convert CAD Geometry into a FloMASTER Sub-System**

**A Study of Aerothermal Loads**

**Development of a Turbocharger with FloEFD**

**Risk Prevention & Energy Saving in Ships**

**Interview: Takuya Shinoda, Denso Corporation**

**Three Thermal Simulation & Test Innovations for Electronics Equipment Design**

**Series Car Brake Cooling**

**Liquid Cooling Turned on its Side**

**Thermal Analysis of an ADAS Camera**

**Thermal Design Leading the Charge**

**Understanding Die Attach Thermal Performance**

**Rapid Beverage Cooling Analysis**

**Bitcoin Mining: A Thermal Perspective**

**Designing High Efficiency, Low-Cost Synchronous Reluctance Motors**

**From Measurements to Standardized Multi-Domain Compact Models of LEDs**

**A Cool Emulator**

**Achieving Precision in 1D Dynamic Models of Hydraulic Servo Valves**

**Using FloEFD as an Engineering Tool**

**Comparison between Experimental & Computational Results**

**Design of a High Speed Decoy UAV**

**Geek Hub: What do Engineers see in Coffee Grounds?**

©2018 Mentor Graphics Corporation, all rights reserved. This document contains information that is proprietary to Mentor Graphics Corporation and may be duplicated in whole or in part by the original recipient for internal business purposes only, provided that this entire notice appears in all copies. In accepting this document, the recipient agrees to make every reasonable effort to prevent unauthorized use of this information. All trademarks mentioned in this publication are the trademarks of their respective owners.